25th DAAAM International Symposium on Intelligent Manufacturing and Automation, DAAAM 2014

Arc Welding Procedures on Steels for Molds and Dies

Sir-Alexci Suarez[a]*, Albert Miyer Suarez[b], Wilson Tafur Preciado[b]

[a]*Department of System Engineering, University Francisco of Paula Santander Ocana, Via Alcosure sede el Algodona, Ocana, 54655, Colombia*
[b]*Faculty of Engineering and Architecture, University of Pamplona, Ciudad Universitaria, Pamplona, Colombia*

Abstract

This work aims to present a method to establish arc welding procedures on steels for molds and dies. The welding of AISI P20 steel was studied. Simple and multi-pass welding were undertaken using the Tungsten inert gas process, evaluating the bead geometry, hardness distribution, microstructure and quality features after grinding, polishing and texturing. By the bead implant test and analytical heat transfer solutions, multi-pass welding techniques were optimized to cause the tempering effect to the weld metal and heat affected zone by a second thermal cycle of welding. In the welding of P20 steel it is necessary to apply the double layer and temper bead techniques. The temper bead demands refined techniques to control the welding variables.

1. Introduction

In the cost of a mold or die, the manufacturing steps are the most expensive, especially with regard to machining and polishing. In general, more than 60% of the total cost corresponds to these steps [1,2]. In such mold repair welding, delicate and expensive procedures must be implemented because of the high manufacturing cost of the component and the need for the rapid availability of the same [3-5].

---

* Corresponding author. Tel.: +57 3006842679.
  E-mail address: sasuarezc@ufpso.edu.co

Plastic injection molds often need to be repaired during manufacture to correct errors in machining or implement changes in component design. The said welds usually affect the characteristics of the uniformity of the finish required on the surfaces after being subjected to polishing and or texturing. It is necessary that the repaired region presents a surface similar to the rest of the mold cavity because otherwise these defects would eventually be reproduced on the molded part [3-5].

Given the influence of the characteristics of steel under the manufacturing conditions and the use of molds and dies, there is much interest in knowing the properties of such machining, polishing and welding. In welding steels that can be hardened, like P20 (traditionally used in the manufacture of molds for plastics) and H13 (used in dies for hot forming), it is necessary to avoid embrittlement and crack formation, mainly related to the formation of retained austenite and martensite [6-8]. In addition, care must be taken in the selection and control of the welding conditions to avoid the generation of high residual stresses and the dimensional distortions they produce.

Traditional methods of minimizing embrittlement in steels and steels that can be hardened, improving the uniformity of the response of these steels to the service requirements, have been the application of preheating and post-welding heat treatment (PWHT). However, thermal treatments are usually expensive and time consuming, not only because of the long residence times of stress relief, but also by the slow heating and cooling ramps that are necessary. Because of this, there is strong motivation to develop technical and economical repair welding procedures, particularly those without PWHT, which ensure acceptable mechanical properties and minimize distortions in the component with optimal performance [9]. With the welding repair techniques without heat treatment after welding, such as double layer and pass tempering, taking advantage of the very heat of the arc to the heat affected zone (HAZ) of the base metal so as to obtain a microstructure suitable to meet the requirements for further treatment and / or service is the aim of the design of the welded component [10].

Nowadays, welding procedures applied in enterprises for the repair of molds and dies are undertaken based on the recommendations given by the manufacturers of the steel, but the metallurgical phenomena involved are not clear to the user, for whom such knowledge is necessary to set judicious procedures suitable for the specific conditions of the material, size and geometry of the mold repair. Most of the information available in the literature on the repair of these steels focuses on aspects of welding techniques without addressing the metallurgical aspects [6,11,12]. Since there are no substitutes for defining procedures for judicious deposition welding in tool steels, in this work a study is made of a steel representative of this problem, the AISI P20. Depending on the application of this steel (plastic injection mold), the welds made using the techniques of double layer and pass tempering are optimally evaluated by observing the response to polishing and texturing treatments.

Through analysis and optimization of the welding deposit conditions of single-pass and multi-pass welding applications of test solutions and cord implantations in a number of heat transfers [13], we tried to reach conditions that would be needed to perform arc welding of tool steels.

2. Materials and Methods

For the tests we used the AISI P20 steel (similar to DIN W.Nr. 1.2738), used for the manufacture of plastic injection molds. It is provided as quenched and tempered, with hardness in the range 30–34 HRC. We used a dissimilar metal addition, AWS A5.28 ER 80S-96-B2, which is a Cr-Mo steel. Table 1 shows the chemical compositions thereof.

Table 1. Chemical composition (weight%) of base and filler metals.

Material	C	Si	Mn	Cr	Ni	Mo	P	S	Cu	Al	Nb	Co	Ti	V
MB	0.37	0.39	1.4	1.89	0.77	0.18	0.03	0.055	0.12	0.002	0.005	0.025	0.002	0.012
MA	0.09	0.58	0.54	1.33	0.04	0.51	0.01	0.006	0.03	-	-	-	-	-

MA=Compositions measured by optical spectrometry.
MB=Compositions provided in the certificate of quality from the manufacturer.

2.1. Simple pass

Table 2 shows the welding parameters adopted using the mechanized Tungsten inert gas (TIG) process. Process conditions were defined according to preliminary practical experiences with AISI P20, using a direct current of constant amplitude (CCC) with preheating of 225 ± 25 ° C [10].

Table 2. TIG process welding conditions.

Current	124 A
Voltage	11 V
Welding speed	10 cm/min
Polarity	CC-
Heat input	10 kJ/cm
Welding arc power	1300 W
Shielding gas	Argon; 12 l/min
Nozzle diameter	10 mm
Electrode de W+ 2%ThO$_2$	Diameter 2.4 mm, tip angle 60°
Arc length	4 mm
Wire diameter	1.2 mm
Wire feed speed	0.5 m/min
Wire incidence angle	25° from plate surface
Torch incidence angle	15° from perpendicular to surface

After depositing this strand on a plate 25 mm thick two CPUs were cut: one intended to analyze the microstructure and hardness measurement in a section transverse to the string and the other prepared for conventional grinding, polishing and etching. The CPUs for metallography and hardness were polished with 13 m sandpaper and 3 micrometer diamond paste. Subsequently they were treated with 2 % Nital solution The Vickers hardness profiles were raised, with a load of 1 kg impressions and spacing of 0.2 mm, in the direction transverse to the cord, including tempered martensite (MS), ZAC and MB. The microstructure was investigated by optical microscopy. Macrograph cross sections of the welds were prepared using a stereoscope. The hardness facilitated the localization of the different regions of the weld. Digital images were entered into Computer-aided design (CAD) software to measure the dimensions of the HAZ of the weld bead (penetration and width of the Ac1 isotherm).

2.2. Optimization and application of multi-pass techniques

To optimize the welding techniques and layered double pass, quenched assay was used to implant a bead, which allows the evaluation of the effect of the produced heat cycle for a second welding pass on the HAZ and MS of the first pass. In this test, a cylindrical sample of the material under study is inserted into a hole speciall in a plate (which may be made of another material) to be flush with the surface. If the thermo physical properties of the material are similar to those of the plate cylinder, the latter suffers the same thermal cycle as the plate, as both are deposited on a weld bead. As a result, all the phenomena associated with the thermal cycle can be portrayed in this small sample (called implants). Fig. 1 shows a schematic of the test.

To analyze the effect of tempering, it is necessary to determine the temperature field peak reached in the welding. This was calculated from the analytical solution produced by Santos [13] for heat transfer that occurs in a solid from a distributed heat source. For this purpose, known temperature processing (e.g. Ac1 determined by dilatometry) and the corresponding isotherm geometry (determined by micrographic analysis, macrographic analysis and second pass in the implant), and calibration of the analytical solutions of heat transfer by adjusting the parameters of the heat source (distribution and thermal efficiency η σ) by solving an inverse problem are undertaken.

We used two computer applications: one to determine the parameters of the heat source according to a known isotherm, and another to determine the temperature distribution in the weld, based on the welding conditions and the parameters of the source. These last values were taken at peak temperature (Tp) to associate them with the values of the hardness measured over certain regions of welding (HAZ -GG and MS of the first pass in the implant) re-heated

for a second welding thermal cycle (produced by the second pass in the implant); thus in this case, providing knowledge of the effect of tempering and position with regard to the Ac1 isotherm. Initially, a semi-circular groove 2 mm in radius was cut into a sheet of about 150x150x25 mm. A cord was deposited in the groove. Cylinders 20 mm in diameter containing a generatrix of the weld bead (Fig. 1) were cut from the welded plates by wire electro-erosion. Fig. 1 shows the scheme for extracting these cylinders. The cylinders were then cut into sections 20 mm long which were embedded with an interference fitted into the holes in the plates of AISI 1020 150x150x21 mm. It also shows the trajectory of the second-pass welding on each inserted cylinder. These cords were made using TIG welding with two autogenous energies (9.8 to 19.6 kJ/cm). To obtain these energies, the set welding speed and the welding current values were maintained at 124 and 248 A.
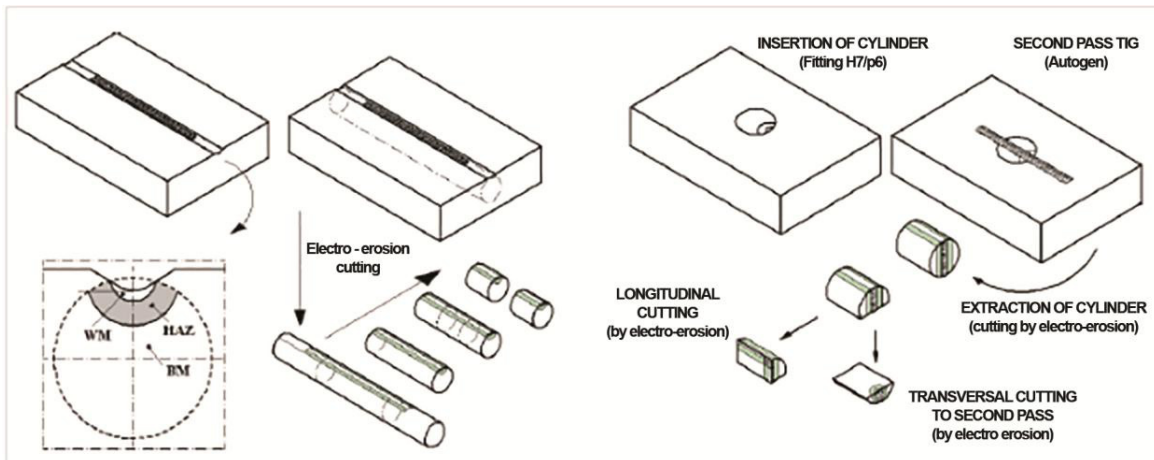

Fig. 1. Bead implant test procedure.

The implant billets, which were attached to the sheet solely by means of the weld bead, were then removed and sectioned by electro-erosion wire as follows: a) across the second weld, bead to bead, macrographs perform the HAZ and determine the temperature field based on the Ac1 isotherm and b) longitudinally to the two weld beads to measure the hardness. The tempering effect produced by the second pass, welding on welding, previously held by the autogenous TIG process, was directly related to the level of energy used in the test cordon, made with wire feed, to obtain the results sought with the multi-pass welding. The implant determined the position of the HAZ produced by the second pass, where the greatest drop in hardness and the MS ZAC first pass occurred. The drop in the HAZ toughness and MS-GG was measured and indicated their position in relation to the Ac1 isotherm to characterize the effect of tempering. On a sheet of 150x150x25 mm a recess, depth of 1 mm with a width of 25 mm and rounded corners, was machined. A layer with 50% overlap between the ridges was deposited in the recess, as shown on the left in Fig. 2. By depositing a second layer, the techniques and tempering of the passes (passes one end, next to MB) were applied to the double layer, using the same welding power in all passes.

All passes were made without oscillation keeping the temperature preheat and interpass at 225 ±25 °C. The cords of the first layer were deposited with 50% overlap. Two CPUs were made, one with 50% overlap and the other with 66% in the second layer. The position of the pass tempering was defined as the distance with respect to the foot of the first and last strands, which should be in the direction of the axis of the tungsten electrode. That position was calculated by simulating the welds in the CAD environment.

The welded plates were cut, rectified, polished and textured. The size of the test specimens was 90 x 45 mm as indicated in Fig. 2. To assess the quality of the textured etched surfaces 10X macrographs were taken, in order to observe the differences in depth of attack.
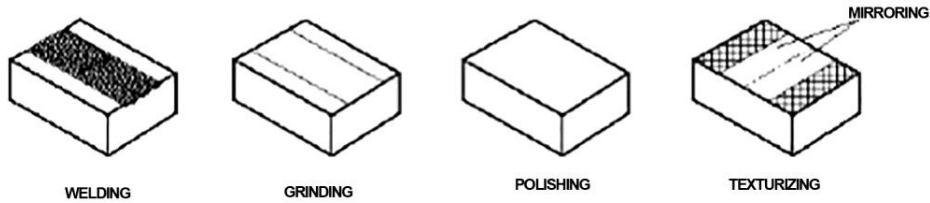
Fig. 2. Specimen for analysis of multi-pass welding.

3. Results

Fig. 3, shows the characteristics of the weld made using sufficient power to avoid the presence of cracks and minor differences in relief after texturing. Even in this condition, the weld on a single pass did not achieve satisfactory quality of the polished and textured surfaces, because the marked differences could be perceived visually.
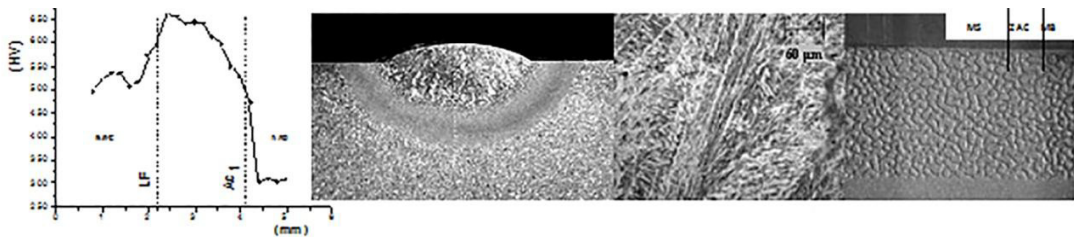

Fig. 3. Characteristics of the single-pass weld AISI P20.

In the MB, due to the annealing treatment prior to formation, carbides occurred in the HAZ and the material was in the tempered martensite with a supersaturated C and other alloying elements. As a result, to obtain a uniform treated surface, it is necessary to promote the tempering of the HAZ and MS, which could be achieved with a conventional heat treatment (with negative effects on the surface finish and dimensional stability) and then through the welding techniques of double layering and pass tempering [10].

The values in the cross section of the implant to the second pass are shown in Table 3. Ali was the isotherm chosen as it was the one with a peak temperature equal to Ac1, which corresponds to the transition between the MB and the ZAC, because it is clearly outlined and because the intention was to study the tempering, which occurs more intensely in temperatures near Ac1 (Fig. 4). For the P20 steel the Ac1 temperature is 780 °C using dilatometry tests.

Table 3. Heat source parameters calculated from isotherm Ac_1.

Energy	Welding Conditions			Isotherm Ac1 Penetration (mm)		Heat Source Parameters	
	Current (A)	Voltage (v)	Welding Speed (cm/min)	HAZ Penetration (mm)	HAZ Width (mm)	Efficiency - η (adim)	Distribution Parameter - σ (mm)
Low	124	11.5	10	4.0	10.0	0.660	1.875
High	248	13.6	10	6.8	17.8	0.620	3.679

Fig. 5 shows the hardness profiles of MS, ZAC-GG (produced by the first pass) and MB functions of the transverse distance in the second pass. Also shown is the Tp curve reached in the second welding cycle, using high (E = 20.23 kJ / cm, η = 62 %) and low energy (E = 8.62 kJ / cm, η = 66 %). The figure shows the profiles of the Ac1 isotherm and the fusion line (LF), observed in the macrographs. The average hardness of the base metal, the

HAZ-GG (coarse grain) and MS before undergoing a second heating were 305, 660 and 600 HV, respectively.

Setting a limit for the final tempering hardness of 450 HV temperature ranges were determined at which the peak tempering effect of the second welding cycle occurs (see Table 4).

Assuming a linear relationship between the energy and the depth of the isotherms, from the data in Table 4 positions of the tempering range limits for the bead deposited with the wire feed were calculated. This allowed the conditions for applying the techniques of double layering and pass tempering to a certain energy to be defined. In this case, for a pass autogenous TIG performed with 7.81 kJ/cm, the places experiencing Tp 600 to 770 °C would be at 4.1 and 5.6 mm from the surface, with Ac1 to 3.8 mm.

As the scale of the simulation passes the welding deposit in the double layer overlap by 50 % (Fig. 6) and observing the diagram in Fig. 5, it was anticipated that the re-heated areas above the Ac1 temperature, the MS, would result in hardness of 500 to 525 HV in the HAZ zone and would be tempered with a hardness of 350 to 450 HV which varies in an alternating manner due to the relatively small overlap of the passes (50%) in the second layer. In the case of an overlap of 66 %, hardness in the range of 350 to 450 HV was expected in all regions (Fig. 6). The results obtained in practice are shown in Fig.7, the hardness profiles corresponding to the pass tempering effects
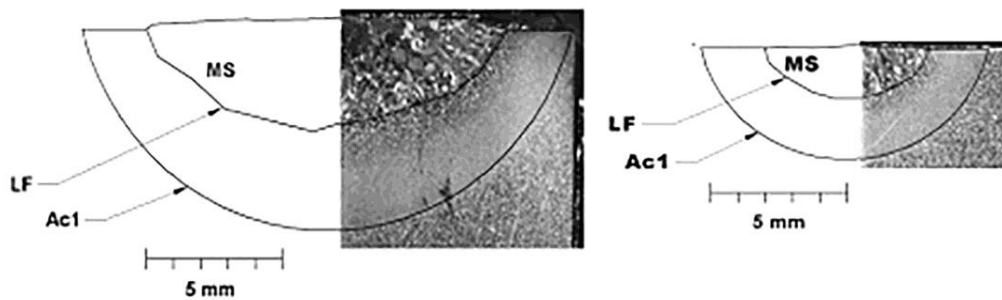

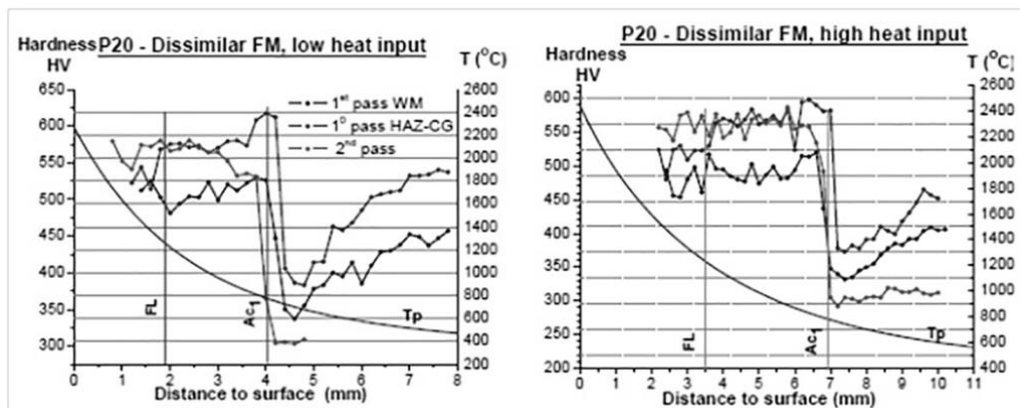Fig. 4. Macrograph cross sections to the 2nd weld bead. Autogenous TIG welding with high and low energy.

Fig. 5. Hardness and temperature profiles peak, the second reached the thermal welding cycle, the regions of the first weld pass.

4. Discussion

In the P20 steel, the regions of the weld produced by a single strand showed great differences in hardness (Fig. 3). Standardization could be accomplished by heat treatment. However, this would result in dimensional changes. By applying the technique of double layering and pass tempering using a high overlap of passes (around 70%) and equal energies for all of them (8 kJ/cm) satisfactory polished and textured surfaces were achieved (Fig. 7). This energy is sufficient to promote the tempering of the HAZ-GG produced in the first layer. On the other hand, when welding with overlapping passes equal to 50%, reliefs and textures in the form of stripes parallel to the cords were

observed on the polished surface as expected. The hardness peak observed in Fig. 7, was due to the difficulty in positioning the pass tempering. For best results, it is necessary to properly position the pass, with a tolerance of a few tenths of a mm, best suited to the application of mechanized welding.

The proposed methodology for the establishment of a multi-pass welding procedure has been shown to be effective by the agreement of the expected results in the simulation and CAD obtained in practice. It also allows estimation of the expected effects by the action of a second thermal cycle of welding over previously deposited beads. It was revealed that at temperatures slightly below the Ac1, tempering occurs and the fall in hardness depends mainly on the peak temperature reached in the second cycle. Such information is a necessary criterion to determine the correct position of the pass and tempering heat input required for the application of the second layer.

Table 4, Tracks of tempering the HAZ-GG and MS from the first pass.

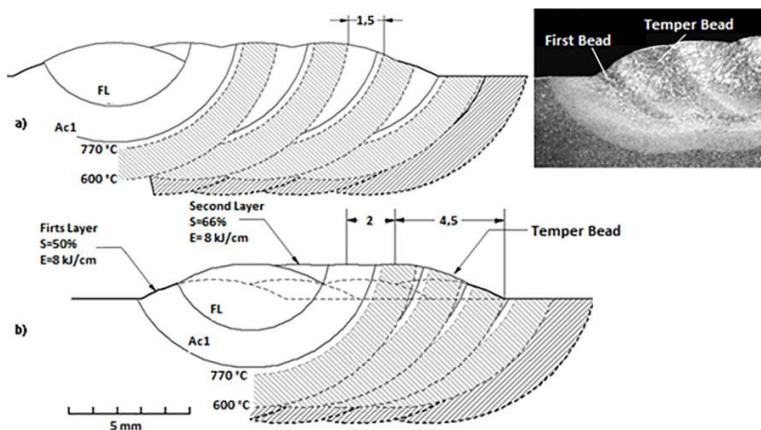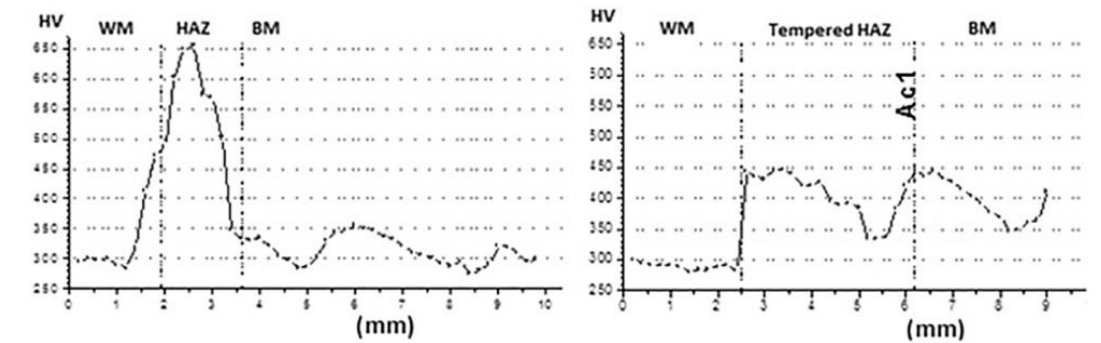|	ZAC-GG 1º pass			MS 1º pass		
Energy	Hardness (HV)	Temperature (ºC)	Distance to sup. the MB (mm)	Hardness (HV)	Temperature (ºC)	Distance to sup. the MB (mm)
Low	370–450	770–600	4.3–5.9	330–450	785–600	4.1–6.1
High	370–450	770–600	7.1–10	330–450	800–600	6.7–10

Fig. 6. Macrograph cross sections of the 1st and 2nd layers. Autogenous TIG welding with high and low energy.
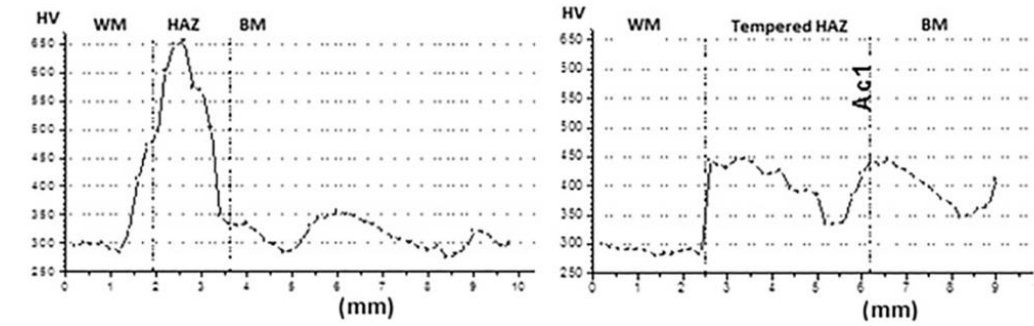
Fig. 7. Hardness profiles in the initial pass of the first and second layer: a) S= 50% ; b) S= 66%.

Conclusions

To get good results in welding AISI P20, it is necessary to properly position the pass tempering and always use high overlapping passes in the second layer with the same welding energy (8 kJ/cm) on all passes to promote the tempering of ZAC-GG in the first layer. Single-pass welding is not recommended to repair the P20 steel, given the differences in hardness and microstructure that MS and ZAC present in relation to the MB, impairing the quality of the mirrored surface and the texture.

Based on the geometric information of the cords deposited with a given energy, it is possible to optimize multi-pass welding techniques solving an inverse problem with the application of test solutions and a number of cord implantations in the heat transfer. It is possible to find conditions where the practice of arc welding tool steels would be needed and predict the characteristics of the weld before it is deposited.

Acknowledgements

References

[1] R.A. Meaquita, C.A. Barbosa, Steels for plastic mold manufacturing with better properties. Proceedings of Machining, Sao Paulo, Out. (2004).
[2] R.A Mesquita, R. Schneider, Tool steel quality and surface finishing of plastic molds, Exacta, 8(2010), 307-318.
[3] W. T. Preciado, C. E. N. Bohorquez: Repair welding of polymer injection molds manufactured in AISI P20 and VP50IM steels, Journal of Materials Processing Technology 179 (2006) 244-250.
[4] A. Skumavic, J. Tusek, M. Mulc, D. Klobcar, Problems in laser repair welding of polished surfaces, Metalurgija 53 (2014) 4, 517-520.
[5] J. Chen, S.H Wang, L. Xue, On the development of microstructures and residual stresses during laser cladding and post-heat treatments. Journal of Materials Science. 47(2012) 779-792.
[6] J. Leunda, V. Garcia, C. Soriano, C. Sanz, Effect of laser tempering of high alloy powder metallurgical tool steels after laser cladding, Surface and Coatings Technology, 259(2014), 570-576
[7] M. Vedani, Microstructural evolution of tool steels after Nd-YAG laser repair welding. Journal of Materials Science, Milan, 39(2004), 241-249.
[8] M. Pleterski,, T. Muhic, D. Klobcar, L. Kosec, Microstructural evolution of a cold, Metalurgija, 51 (2012) 1, 13-16.
[9] Bueno, E.: Development of Welding Procedure of AISI 4140 without Heat Treatment Posterior.. 74p. Master's Dissertation, Graduate Program in Mechanical Engineering, Federal University of Santa Catarina, Florianopolis (1999).
[10] Nino, C.E.: "Specification of procedures for repair welding without subsequent heat treatment: effect of tempering produced by thermal cycling". PhD thesis, Graduate Program in Mechanical Engineering, Federal University of Santa Catarina, Florianópolis (2001).
[11] Thompson, S.: Handbook of mould, tool and die repair welding. 1. ed. Abington Publishing Limited. 224p. (1999).
[12] Takagi, R.: Repair welding for plastic injection mold. Tool Steels, Tokio, 68, 95–104 (1997).
[13] Santos, L.: "Heat conduction welding with thermal pulse". PhD thesis, Graduate Program in Mechanical Engineering, Federal University of Santa Catarina, Florianópolis (2001).